

# Troubles of describing multiple pion production in chiral dynamics

N. N. Achasov<sup>a\*</sup>, A. A. Kozhevnikov<sup>a,b†</sup>

<sup>a</sup> *Laboratory of Theoretical Physics, S. L. Sobolev Institute for Mathematics  
630090, Novosibirsk, Russian Federation*

<sup>b</sup> *Novosibirsk State University  
630090, Novosibirsk, Russian Federation*

## Abstract

Generalized Hidden Local Symmetry (GHLS) model as the chiral model of pseudoscalar, vector, and axial vector mesons and their interactions containing also the couplings of strongly interacting particles with electroweak gauge bosons, is confronted with the ALEPH data on the decay  $\tau^- \rightarrow \pi^- \pi^- \pi^+ \nu_\tau$  and BABAR and CMD data on the reaction  $e^+e^- \rightarrow \pi^+ \pi^- \pi^+ \pi^-$ . It is shown that both the invariant mass spectrum of final pions in  $\tau$  decay calculated in the GHLS framework with the single  $a_1(1260)$  resonance and the cross section  $e^+e^- \rightarrow \pi^+ \pi^- \pi^+ \pi^-$  calculated in the above framework with the single  $\rho(770)$  resonance, disagree with the experimental data. The modifications of GHLS model based on inclusion of two additional heavier axial vector mesons  $a'_1$ ,  $a''_1$  in the  $\tau$  decay and the vector mesons  $\rho'$ ,  $\rho''$  in  $e^+e^- \rightarrow \pi^+ \pi^- \pi^+ \pi^-$  are shown to be necessary for the good description of the above data.

**1. Introduction.** The theory aimed at describing low energy hadron processes should be formulated in terms of effective colorless degrees of freedom introduced on the basis of spontaneously broken approximate chiral symmetry  $SU(3)_L \times SU(3)_R$ . This is the symmetry of QCD Lagrangian

$$\mathcal{L}_{\text{QCD}} = -\frac{1}{4} \left( \partial_\mu G_\nu^a - \partial_\nu G_\mu^a + g f_{abc} G_\mu^b G_\nu^c \right)^2 + \sum_q \bar{q} \left[ \gamma_\mu \left( i \partial_\mu - g \frac{\lambda^a}{2} G_{a\mu} \right) - m_q \right] q, \quad (1)$$

relative independent rotations of right and left fields of approximately massless  $u, d, s$  quarks:

$$q_L \equiv \frac{1 + \gamma_5}{2} q \rightarrow V_L q_L, \quad q_R \equiv \frac{1 - \gamma_5}{2} q \rightarrow V_R q_R, \quad (2)$$

where  $V_{L,R} \in SU(3)_{L,R}$ . The pattern of the spontaneous breaking is  $SU(3)_L \times SU(3)_R \Rightarrow SU(3)_{L+R}$ . According to the Goldstone theorem, spontaneous breaking of global symmetry results in appearance of massless fields. In our case they are light  $J^P = 0^-$  mesons  $\pi^+$ ,  $\pi^-$ ,  $\pi^0$ ,  $K^+$ ,  $K^0$ ,  $K^-$ ,  $\bar{K}^0$ ,  $\eta$ . The transformation law  $U \rightarrow V_L U V_R^\dagger$  where  $U = \exp(i\Phi\sqrt{2}/f_\pi)$ , and

$$\Phi = \begin{pmatrix} \frac{\pi^0}{\sqrt{2}} + \frac{\eta}{\sqrt{6}} & \pi^+ & K^+ \\ \pi^- & -\frac{\pi^0}{\sqrt{2}} + \frac{\eta}{\sqrt{6}} & K^0 \\ K^- & \bar{K}^0 & -\frac{2\eta}{\sqrt{6}} \end{pmatrix}, \quad (3)$$

fixes the Lagrangian of interacting Goldstone mesons:

$$\mathcal{L}_{\text{GB}} = \frac{f_\pi^2}{4} \text{Sp} \left( \partial_\mu U \partial_\mu U^\dagger \right) + \dots$$

---

\*e-mail: achasov@math.nsc.ru

†e-mail: kozhev@math.nsc.ru

Dots mean the terms with higher derivatives. Upon adding the term  $\propto m_\pi^2 \text{Sp}(U + U^\dagger)$  which explicitly breaks chiral symmetry, Goldstone bosons become massive.

Pseudoscalar mesons are produced via intermediate vector and axial resonances, hence one should include vector and axial vector mesons in a chiral invariant way. There are a number of chiral models of pseudoscalar, vector, and axial mesons and their interaction [1]. The problem of testing chiral models of the vector meson interactions with Goldstone bosons is acute. The present report is devoted to reviewing the attempts to confront one of the chiral models, the Generalized Hidden Local Symmetry (GHLS) model [2, 3, 4], with the data on the decay  $\tau^- \rightarrow \pi^+ \pi^- \pi^- \nu_\tau$  [5] in the axial vector channel, and the data on the reaction  $e^+ e^- \rightarrow \pi^+ \pi^- \pi^+ \pi^-$  [6, 7] in the vector channel, both in the state with the isospin one.

**2. Generalized Hidden Local Symmetry Model Lagrangian.** The Generalized Hidden Local Symmetry (GHLS) model [2, 3, 4] as the chiral model based on nonlinear realization of chiral symmetry, is of a special interest because some interesting two- and three-particle decays, for example,  $\rho^0 \rightarrow \pi^+ \pi^-$  and  $\omega \rightarrow \pi^+ \pi^- \pi^0$ , were analyzed in its framework [4]. "Hidden" means that if  $U = \xi_L^\dagger \xi_R$  then the transformation law  $\xi_{L,R} \rightarrow h \xi_{L,R} g_{L,R}^\dagger$  implies one  $U \rightarrow g_L U g_R^\dagger$  where  $h$  transforms vector meson fields in a gauge-like manner as  $V_\mu \rightarrow h V_\mu h^\dagger - i \partial_\mu h h^\dagger$ . "Generalized hidden" means that axial vector mesons are included. One of the virtues of GHLS model is that the sector of electroweak interactions is introduced in such a way that the low energy relations in the sector of strong interactions are not violated upon inclusion of photons and electroweak gauge bosons. The GHLS lagrangian includes pseudoscalar, vector, and axial vector fields  $\xi$ ,  $V_\mu$ , and  $A_\mu$ , respectively. In the gauge  $\xi_M = 1$ ,  $\xi_L^\dagger = \xi_R = \xi$  and after rotating away the axial vector- $\pi$  mixing by choosing

$$A_\mu = a_\mu - \frac{b_0 c_0}{g(b_0 + c_0)} A_{(\xi)\mu}, \quad (4)$$

where  $a_\mu$  is  $a_1$  meson field,  $g$  is the coupling constant to be related to  $g_{\rho\pi\pi}$ , and

$$A_{(\xi)\mu} = \frac{\partial_\mu \xi^\dagger \xi - \partial_\mu \xi \xi^\dagger}{2i}, \quad (5)$$

the relevant terms corresponding to strong interactions look like

$$\begin{aligned} \mathcal{L}_{\text{strong}} = & a_0 f_\pi^{(0)2} \text{Tr} \left( \frac{\partial_\mu \xi^\dagger \xi + \partial_\mu \xi \xi^\dagger}{2i} - g V_\mu \right)^2 + f_\pi^{(0)2} \left( d_0 + \frac{b_0 c_0}{b_0 + c_0} \right) \text{Tr} A_{(\xi)\mu}^2 + \\ & (b_0 + c_0) f_\pi^{(0)2} g^2 \text{Tr} a_\mu^2 + d_0 f_\pi^{(0)2} \text{Tr} A_{(\xi)\mu}^2 - \frac{1}{2} \text{Tr} \left( F_{\mu\nu}^{(V)2} + F_{\mu\nu}^{(A)2} \right) - \\ & i \alpha_4 g \text{Tr} [A_\mu, A_\nu] F_{\mu\nu}^{(V)} + 2i \alpha_5 \text{Tr} \left( [A_{(\xi)\mu}, A_\nu] + g [A_\mu, A_\nu] \right) F_{\mu\nu}^{(V)}. \end{aligned} \quad (6)$$

The lagrangian contains a number of free parameters  $a_0, b_0, c_0, d_0, \alpha_4, \alpha_5$ . The terms with free parameters  $\alpha_{4,5}$  are necessary for cancelation of momentum dependence in the  $\rho\pi\pi$  vertex. They are chosen in accord with Refs. [3, 4] in such a way that among the terms with higher derivatives those with  $\alpha_1, \alpha_2, \alpha_3$  are set to zero, and only the  $\alpha_{4,5,6}$  terms are included, with the additional assumption  $\alpha_5 = \alpha_6$  about the arbitrary constants multiplying the lagrangian terms. The remaining ones  $\alpha_4$  and  $\alpha_5$  should be related like

$$\alpha_4 = 1 - \frac{2\alpha_5 c_0}{b_0}, \quad (7)$$

in order to provide the desired cancelation. The notations, assuming the restriction to the sector of the non-strange mesons, are

$$\begin{aligned} F_{\mu\nu}^{(V)} &= \partial_\mu V_\nu - \partial_\nu V_\mu - ig[V_\mu, V_\nu] - ig[A_\mu, A_\nu], \\ F_{\mu\nu}^{(A)} &= \partial_\mu A_\nu - \partial_\nu A_\mu - ig[V_\mu, A_\nu] - ig[A_\mu, V_\nu], \\ V_\mu &= \left( \frac{\boldsymbol{\tau}}{2} \cdot \boldsymbol{\rho}_\mu \right), \quad A_\mu = \left( \frac{\boldsymbol{\tau}}{2} \cdot \mathbf{A}_\mu \right), \quad \xi = \exp i \frac{\boldsymbol{\tau} \cdot \boldsymbol{\pi}}{2f_\pi^{(0)}}, \end{aligned} \quad (8)$$

where  $\boldsymbol{\rho}_\mu$ ,  $\boldsymbol{\pi}$  are the vector meson  $\rho$  and pseudoscalar pion fields, respectively,  $\mathbf{A}_\mu$  is the axial vector field [not  $a_1$  meson, see Eq. (4)],  $\boldsymbol{\tau}$  is the isospin Pauli matrices. Free parameters ( $a_0, b_0, c_0, d_0$ ), and  $f_\pi^{(0)}$  of the GHLS lagrangian with index 0 are bare parameters before renormalization (see below);  $[\cdot, \cdot]$  stands for commutator. Hereafter the boldface characters, cross ( $\times$ ), and dot ( $\cdot$ ) stand for vectors, vector product, and scalar product, respectively, in the isotopic space.

GHLS lagrangian includes also electroweak sector. In what follows we will neglect the terms quadratic in electroweak coupling constants keeping only the terms linear in above couplings. These terms describe the interaction of  $\pi$ ,  $\rho$ , and  $a_1$  mesons with electroweak gauge bosons and look as [3, 4]

$$\Delta\mathcal{L}_{\text{EW}} = 2f_\pi^{(0)2}\bar{g}\text{Tr}\left\{a_0\left(\frac{\partial_\mu\xi^\dagger\xi + \partial_\mu\xi\xi^\dagger}{2i}\frac{\xi^\dagger\mathcal{L}_\mu\xi + \xi\mathcal{R}_\mu\xi^\dagger}{2}\right) + \left(d_0 + \frac{b_0c_0}{b_0+c_0}\right)\times\right. \\ \left.A_{(\xi)\mu}\frac{\xi^\dagger\mathcal{L}_\mu\xi - \xi\mathcal{R}_\mu\xi^\dagger}{2} - a_0gV_\mu\frac{\xi^\dagger\mathcal{L}_\mu\xi + \xi\mathcal{R}_\mu\xi^\dagger}{2} + b_0ga_\mu\frac{\xi^\dagger\mathcal{L}_\mu\xi - \xi\mathcal{R}_\mu\xi^\dagger}{2}\right\}. \quad (9)$$

Upon neglecting the weak neutral current contribution, the charged weak and electromagnetic sectors are taken into account via [3, 4],

$$\bar{g}\mathcal{L}_\mu = \frac{g_2}{\sqrt{2}}(W_\mu^+T_- + W_\mu^-T_+) + eQ\mathcal{A}_\mu, \quad \bar{g}\mathcal{R}_\mu = eQ\mathcal{A}_\mu, \quad (10)$$

$W_\mu^\pm$  are the fields of  $W^\pm$  bosons,  $g_2$  is the electroweak  $SU(2)$  gauge coupling constant. In the  $SU(2)$  subgroup of the flavor  $SU(3)$  group of strong interactions one has  $T^+ = \begin{pmatrix} 0 & V_{ud} \\ 0 & 0 \end{pmatrix}$ ,  $V_{ud} = \cos\theta_C$  is the element of Cabibbo-Kobayashi-Maskawa matrix,  $\mathcal{A}_\mu$  stands for the field of the photon,  $e$  is the elementary charge, and  $Q = \frac{1}{3}\begin{pmatrix} 2 & 0 \\ 0 & -1 \end{pmatrix}$  is the charge matrix restricted to the sector of nonstrange mesons. In the spirit of chiral perturbation theory, as the first step in obtaining necessary terms, one should expand the matrix  $\xi$  into the series over  $\boldsymbol{\pi}/f_\pi^{(0)}$ . The second step is the renormalization necessary for canonical normalization of the pion kinetic term. The renormalization is [3, 4]

$$f_\pi^{(0)} = Z^{-1/2}f_\pi, \boldsymbol{\pi} \rightarrow Z^{-1/2}\boldsymbol{\pi}, (a_0, b_0, c_0, d_0) = Z \times (a, b, c, d), \quad (11)$$

where  $\left(d_0 + \frac{b_0c_0}{b_0+c_0}\right)Z^{-1} = 1$ . Close examination of Eq. (9) shows that the expansion includes the point-like interaction  $\left(\frac{a}{2} - d - \frac{bc}{b+c}\right)W_\mu^-[\boldsymbol{\pi} \times \partial_\mu\boldsymbol{\pi}]_{1+i2}$ . Analogous term appears when one restores electromagnetic field. Since there are no experimental indications on point-like  $\gamma \rightarrow \pi^+\pi^-$  vertex, we set

$$\frac{a}{2} - d - \frac{bc}{b+c} = 0. \quad (12)$$

This relation removes also the above point-like  $W^- \rightarrow \pi^-\pi^0$  vertex.

**3. The amplitude of the transition  $W^- \rightarrow 2\pi^-\pi^+$ .** Expanding the GHLS lagrangian into the series in the ratio of the pion momentum to the pion decay constant  $f_\pi = 92.4$  MeV, first, one obtains the relations

$$g_{\rho\pi\pi} = \frac{ag}{2}, m_\rho^2 = ag^2f_\pi^2, m_{a_1}^2 = (b+c)g^2f_\pi^2. \quad (13)$$

We fix hereafter  $g_{\rho\pi\pi}$  from the experimental value of the  $\rho^0 \rightarrow \pi^+\pi^-$  decay width leaving  $a$  as free parameter. Second, the lagrangian describing the decay  $a_1 \rightarrow 3\pi$  is found to be

$$\mathcal{L}_{a_13\pi} = -\frac{r}{f_\pi}(\partial_\mu\mathbf{a}_\nu - \partial_\nu\mathbf{a}_\mu)[\boldsymbol{\rho}_\mu \times \partial_\nu\boldsymbol{\pi}] + \frac{\alpha_5}{f_\pi}\mathbf{a}_\mu[(\partial_\mu\boldsymbol{\rho}_\nu - \partial_\nu\boldsymbol{\rho}_\mu) \times \partial_\nu\boldsymbol{\pi}] - \\ \frac{r^2}{2gf_\pi^3}(\alpha_5 - r)[\mathbf{a}_\mu \times \partial_\nu\boldsymbol{\pi}] \cdot [\partial_\mu\boldsymbol{\pi} \times \partial_\nu\boldsymbol{\pi}] - \frac{r}{2gf_\pi^3}\partial_\mu\mathbf{a}_\nu \cdot [\boldsymbol{\pi} \times [\partial_\mu\boldsymbol{\pi} \times \partial_\nu\boldsymbol{\pi}]]. \quad (14)$$

The amplitude of the decay  $a_1^-(q) \rightarrow \pi^+(q_1)\pi^-(q_2)\pi^-(q_3)$  calculated from Eq. (14) can be written as follows:  $M[a_1^-(q) \rightarrow \pi^+(q_1)\pi^-(q_2)\pi^-(q_3)] \equiv M_{a_1 3\pi}$ ,

$$iM_{a_1 3\pi} = \frac{agr}{2f_\pi} \epsilon_\mu (A_1 q_{1\mu} + A_2 q_{2\mu} + A_3 q_{3\mu}), \quad (15)$$

where  $\epsilon_\mu$  is the polarization four-vector of  $a_1$  meson, and  $A_1 = (1 + \hat{P}_{23})\tilde{A}_1$ , where

$$\begin{aligned} \tilde{A}_1 &= \frac{\beta[(q_3, q_1 - q_2) - (q, q_3) + m_\pi^2] - (q, q_3)}{D_\rho(q_1 + q_2)} + \frac{4r^2(\beta - 1)(q_2, q_3) + (q, q) - (q, q_1)}{2m_\rho^2}, \\ A_2 &= \frac{\beta[(q_3, q_1 - q_2) + (q, q_3) - m_\pi^2] + (q, q_3)}{D_\rho(q_1 + q_2)} + \frac{(q_2, q_1 - q_3)}{D_\rho(q_1 + q_3)} - \frac{2r^2(\beta - 1)(q_1, q_3) + (q, q_1)}{m_\rho^2}. \end{aligned}$$

Hereafter  $\hat{P}_{ij}$  interchanges pion momenta  $q_i$  and  $q_j$ ,  $(q_i, q_j)$  stands for the Lorentz scalar product of four-vectors, and  $A_3 = \hat{P}_{23}A_2$ . Parameters  $r$  and  $\beta$  are the combinations of the GHLS parameters:

$$r = \frac{b}{b+c}, \quad \beta = \frac{\alpha_5}{r}. \quad (16)$$

Notice that the amplitude (15) respects the Adler condition: it vanishes in the chiral limit  $m_\pi^2 \rightarrow 0$  when the four-momentum of any final pion vanishes. Such a property is the manifestation of the chiral invariance.

The amplitude of the decay  $\tau^- \rightarrow \pi^- \pi^- \pi^+ \nu_\tau$  incorporates the transition  $W^- \rightarrow \pi^- \pi^- \pi^+$ . In GHLS, the latter is given by the diagrams shown in Fig. 1. Necessary terms are obtained from the low momentum expansion of electroweak piece of GHLS lagrangian Eq. (9) and look like

$$\begin{aligned} \Delta\mathcal{L}_{EW} &= \frac{1}{2}g_2 V_{ud} \mathbf{W}_\mu \cdot \left( -f_\pi \partial_\mu \boldsymbol{\pi}_\perp + \frac{1}{3f_\pi} [\boldsymbol{\pi} \times [\boldsymbol{\pi} \times \partial_\mu \boldsymbol{\pi}]]_\perp + bgf_\pi^2 \mathbf{a}_\mu \cdot \boldsymbol{\pi}_\perp + agf_\pi [\boldsymbol{\pi} \times \boldsymbol{\rho}_\mu]_\perp \right) \\ &\quad - eg\mathcal{A}_\mu \left\{ a\rho_\mu^0 (f_\pi^2 - \pi^+ \pi^-) - \frac{2\pi^+ \pi^-}{3gf_\pi^2} [\boldsymbol{\pi} \times \partial_\mu \boldsymbol{\pi}]_3 \left( \frac{7}{8}a - rc \right) + bf_\pi [\boldsymbol{\pi} \times \mathbf{a}_\mu]_3 \right\}, \quad (17) \end{aligned}$$

where the vector  $\mathbf{V}_\perp = (V_1, V_2)$  denotes transverse charged components of the isotopic vector. The amplitude of the decay  $W^-(q) \rightarrow \pi^+(q_1)\pi^-(q_2)\pi^-(q_3)$  corresponding to the diagrams Fig. 1 is  $iM = \frac{g_2 V_{ud}}{2f_\pi} \epsilon_\mu^{(W)} J_\mu$ , where  $\epsilon_\mu^{(W)}$  is the polarization four-vector of  $W^-$  boson and the axial decay current  $J_\mu$  looks like

$$\begin{aligned} J_\mu &= -q_{1\mu} + \frac{q_\mu}{D_\pi(q)} \left[ m_\pi^2 - (q, q_1) + \frac{am_\rho^2}{2} (1 + \hat{P}_{23}) \frac{(q_2, q_1 - q_3)}{D_\rho(q_1 + q_3)} \right] - \frac{ar^2 m_{a_1}^2}{2D_{a_1}(q)} \times \\ &\quad \left\{ A_1 q_{1\mu} + A_2 q_{2\mu} + A_3 q_{3\mu} - \frac{2q_\mu}{m_{a_1}^2} (1 + \hat{P}_{23}) [(m_\pi^2 + (q_1, q_2))(q_3, q_1 - q_2) \times \right. \\ &\quad \left. \left( \frac{\beta}{D_\rho(q_1 + q_2)} - \frac{r^2(\beta - 1)}{m_\rho^2} \right) \right] \right\} + \frac{am_\rho^2}{2} (1 + \hat{P}_{23}) \frac{(q_1 - q_3)_\mu}{D_\rho(q_1 + q_3)}. \quad (18) \end{aligned}$$

In the above expressions,  $D_\rho$ ,  $D_\pi$ , and  $D_{a_1}$  are the inverse propagators of  $\pi$ ,  $\rho$ , and  $a_1$  mesons, respectively. The terms corresponding to the diagrams (a), (b), (c), and (d) in Fig. 1 are easily identified by these propagators.

The spectrum of the three pion state in the decay  $\tau^- \rightarrow \pi^+ \pi^- \pi^- \nu_\tau$  normalized to its branching fraction is

$$\frac{dB}{ds} = \frac{(G_F V_{ud})^2 (m_\tau^2 - s)^2}{2\pi (2m_\tau)^3 \Gamma_\tau} [(m_\tau^2 + 2s)\rho_t(s) + m_\tau^2 \rho_l(s)], \quad (19)$$

$s = q^2$ ,  $G_F$  is the Fermi constant, and  $\Gamma_\tau$  is the width of  $\tau$  lepton. The transverse and longitudinal spectral functions are, respectively,

$$\rho_t(s) = \frac{1}{3\pi s f_\pi^2} \int d\Phi_{3\pi} \left[ \frac{|(q, J)|^2}{s} - (J, J^*) \right], \quad \rho_l(s) = \frac{1}{\pi s^2 f_\pi^2} \int d\Phi_{3\pi} |(q, J)|^2, \quad (20)$$

where  $d\Phi_{3\pi}$  is the element of Lorentz-invariant phase space volume of the system  $\pi^- \pi^- \pi^+$ . The numerical integration shows that  $\rho_l$  is by about three orders of magnitude smaller than  $\rho_t$  in all allowed kinematical range  $9m_\pi^2 < s < m_\tau^2$  and hence can be neglected.

**4. Results for  $\tau^- \rightarrow \pi^+ \pi^- \pi^- \nu_\tau$ .** The "canonical" choice of free GHLS parameters [4]

$$(a, b, c, d, \alpha_4, \alpha_5, \alpha_6) = (2, 2, 2, 0, -1, 1, 1), \quad (21)$$

and  $\alpha_1 = \alpha_2 = \alpha_3 = 0$ , results in the spectrum which disagrees with the data both in lower branching ratio  $B_{\tau^- \rightarrow \pi^+ \pi^- \pi^- \nu_\tau} \approx 6\%$  and in the shape of the spectrum. Upon the variation of free parameters of the single  $a_1$  resonance contribution listed in Eq. (21) one obtains the can reproduce the branching ratio  $B_{\tau^- \rightarrow \pi^+ \pi^- \pi^- \nu_\tau} \approx 9\%$  but the shape of the spectrum is not reproduced. Inclusion of additional higher derivative terms to the suggested in Refs. [3, 4] minimal set Eq. (21) and subjected to the fitting in the present work cannot improve the situation. Indeed, even the minimal set Eq. (21) results in a rather fast growth of the  $a_1 \rightarrow 3\pi$  decay width with the energy increase. Additional higher derivative terms would make the growth to be explosive. Restricting such a growth would require phenomenological form factors with free parameters. We believe that the dynamical explanation of the shape of the spectrum based on additional axial vector resonances  $a'_1$ ,  $a''_1$  would be preferable. Note that there are indications on such resonances, both theoretical [8, 9] and experimental [10, 11, 12].

Taking  $a'_1$ ,  $a''_1$  into account reduces to adding two diagrams similar to one in Fig. 1(c), with the replacement of  $a_1(1260)$  by  $a'_1$  and  $a''_1$ . Since there is no available information concerning their couplings, the above resonances are included in a way analogous to  $a_1(1260)$ . This prescription results in the amplitudes of the decays  $a'_1, a''_1 \rightarrow 3\pi$  vanishing when the four-momentum of any final pion vanishes. That is, the way of inclusion additional resonances respects chiral symmetry. The total set of the fitted parameters is first taken to be

$$(m_{a_1}, a, r, \beta, m_{a'_1}, a', r', \beta', w', m_{a''_1}, a'', r'', \beta'', w'').$$

The parameters  $a', r', \beta'$  characterize the  $a'_1 \rightarrow 3\pi$  decay amplitude similar to Eq. (15), (16) in the case of  $a_1(1260) \rightarrow 3\pi$ , while  $w'$  parameterizes the coupling  $a'_1 \rho \pi$  as  $g_{\rho\pi\pi} w' r' / f_\pi$ . Compare with Eq. (15). Analogously for  $a''_1$ . The fit chooses  $w' = 1$  and turns out to be insensitive to this parameter leaving  $\chi^2/N_{\text{d.o.f}} = 122/102$ . The quality of the fit can be considerably improved upon fixing  $w' = 1$  but adding new parameter  $\psi'$ -the phase of the  $a'_1$  contribution. Such phase imitates possible mixing among  $a_1$ ,  $a'_1$ ,  $a''_1$  resonances. The results of such type of the fit are given in the column variant A of the Table 1. The corresponding spectrum is shown in Fig. 2. Using Eq. (13), (16), and obtaining  $g_{\rho\pi\pi} = 5.95$  from  $\Gamma_{\rho\pi\pi}$  [10] one can compare the fitted GHLS parameters with the "canonical" ones Eq. (21). To this end one should use Eq. (12) and (13) to obtain

$$\begin{aligned} b &= r \left( \frac{m_{a_1} a}{2f_\pi g_{\rho\pi\pi}} \right)^2, \quad c = (1-r) \left( \frac{m_{a_1} a}{2f_\pi g_{\rho\pi\pi}} \right)^2, \quad d = \frac{a}{2} - r(1-r) \left( \frac{m_{a_1} a}{2f_\pi g_{\rho\pi\pi}} \right)^2, \\ \alpha_4 &= 1 - 2\beta(1-r), \quad \alpha_5 = \beta r, \quad \alpha_6 = \alpha_5. \end{aligned} \quad (22)$$

These GHLS parameters are marked in the Table 1 as "calculated". Since the basis of inclusion of heavier resonances  $a'_1$  and  $a''_1$  here is purely phenomenological, specifically, there is no analog of gauge coupling constant  $g$ , we do not recalculate  $(a', b', c', d', \dots)$  and  $(a'', b'', c'', d'', \dots)$  similar to Eq. (22). One can see that the obtained  $a = 1.665 \pm 0.011$  is in disagreement with

the universality condition  $g_{\rho\pi\pi} = g$ , which demands  $a = 2$ , see Eq. (13). Hence we fulfill also the partially constrained fit with  $a \equiv 2$ , in order to preserve universality of the  $\rho$  couplings. The results are presented as the variant B in the Table 1. The total spectrum in this variant is not shown because it looks the same as in Fig. 2. Note that in the variant A the visible  $a_1''$  peak position is lower than that of  $a_1'$  despite of the fact that their bare masses are in opposite relation, see the Table 1. This can be explained as follows. The dominant decay mode of  $a_1'$ ,  $a_1''$  resonances is the  $3\pi$  one. Its partial width grows rapidly with energy increase reaching the figures compatible with bare mass itself. The combined action of the strong energy dependence of the partial width and its large magnitude shifts the visible peak towards the lower energies [14]. The evaluation shows that the width of  $a_1''$  and its growth are stronger as compared to  $a_1'$ . Hence the visible position of the former appears at lower energy than the visible position of  $a_1'$ .

Of a special interest is the width of the radiative decay  $a_1^\pm \rightarrow \pi^\pm\gamma$ . This decay originates from both the  $a_1 \rightarrow \rho\pi$  transition followed by the transition  $\rho \rightarrow \gamma$  and by the direct  $a_1 \rightarrow \pi\gamma$  transition. The necessary amplitudes can be read off Eq. (17). The resulting  $a_1^\pm \rightarrow \pi^\pm\gamma$  decay width is

$$\Gamma_{a_1^\pm \rightarrow \pi^\pm\gamma} = \frac{\alpha a m_{a_1}^3}{24 m_\rho^2} [r(\beta - 1)]^2 \left(1 - \frac{m_\pi^2}{m_{a_1}^2}\right)^3, \quad (23)$$

where  $\alpha$  is the fine structure constant. Notice, that the above expression for  $\Gamma_{a_1^\pm \rightarrow \pi^\pm\gamma}$  is written with the counter terms taken into account. The  $a_1^\pm \rightarrow \pi^\pm\gamma$  decay amplitude without counter terms is proportional to the combination  $b - a r m_{a_1}^2 / m_\rho^2$  which vanishes at any choice of GHLS parameters because of the relations (13) and (16). The evaluation of  $\Gamma_{a_1^\pm \rightarrow \pi^\pm\gamma}$  with the parameters from the variants A and B of the Table 1 gives the figures of the order of few MeV due to large values of  $\beta$  in the Table 1 chosen by the fits. This is in disagreement with the measured  $\Gamma_{a_1^\pm \rightarrow \pi^\pm\gamma} = 640 \pm 246$  keV [13]. Hence, one should further constrain the fit in order to incorporate the above radiative width upon expressing parameter  $\beta$  from Eq. (23). When fitting, the central value of the  $a_1(1260)$  radiative width. To provide the universality of the  $\rho$  couplings,  $a = 2$  is kept fixed, too. It is found out that the fit with the fixed parameters  $a$  and  $\beta$  gives rather poor description with  $\chi^2/N_{\text{d.o.f}} = 209/102$ . The peculiar feature of the fit is that it chooses  $\psi' \approx 0$ , the phase of the  $a_1'$  contribution, but  $\chi^2$  is almost insensitive to the rather wide variations around above central value. Hence, we fix  $\psi' \equiv 0$ , but introduce a new free parameter  $\gamma$  whose meaning is  $\gamma = m_{a_1} \Delta\Gamma_{a_1}$ , where  $\Delta\Gamma_{a_1}$  effectively takes into account the contributions to the  $a_1$  resonance width other than  $\rho\pi + 3\pi \rightarrow 3\pi$  one, for example,  $a_1 \rightarrow \rho'\pi \rightarrow 3\pi$ ,  $K\bar{K}\pi$ . They may be effective for the off-mass-shell  $a_1$  meson. The results of such type of the fit are presented as the variant C in the Table 2. The spectrum of the system  $\pi^+\pi^-\pi^+\pi^-$  evaluated with the parameters of variant C is shown with the solid line in Fig. 3. Note that the found  $\gamma = m_{a_1} \Delta\Gamma_{a_1} \sim 0.3$  GeV<sup>2</sup> corresponds to the portion of the  $a_1$  decay channels different from  $\rho\pi + 3\pi \rightarrow 3\pi$  one, at the level  $\Delta\Gamma_{a_1} / \Gamma_{a_1 \rightarrow 3\pi} \sim 0.02$ . This estimate can be obtained from the calculated  $\Gamma_{a_1 \rightarrow \rho\pi + 3\pi \rightarrow 3\pi}$ . The above estimate demonstrates that the additional contribution to the  $a_1$  width beside the GHLS one is very small. Since the contribution of the resonance  $a_1''$  is rather small, see Fig. 3, we fulfill the fit in which the contribution of the resonance is absent. The parameters found in such type of the fit are listed as the variant D in the Table 2.

**5. GHLS and the reaction  $e^+e^- \rightarrow \pi^+\pi^-\pi^+\pi^-$  at  $\sqrt{s} \leq 1$  GeV.** Because the evaluation of the four pion decay width of the  $\rho$ -like resonances is very time-consuming, we study the predictions of GHLS model for the reaction  $e^+e^- \rightarrow \pi^+\pi^-\pi^+\pi^-$  with the "canonical" choice of free parameters (21). The set of the diagrams necessary for calculation of the amplitude is shown in Fig. 4, 5, and 6. This set includes the resonance production  $e^+e^- \rightarrow R \rightarrow \pi^+\pi^-\pi^+\pi^-$ , where  $R = \rho, \rho', \rho''$  (see below), and the point-like transitions due to the GHLS electromagnetic coupling (17) where free GHLS parameters are chosen in accord with (21).

The results of evaluation of the cross section of the reaction  $e^+e^- \rightarrow \pi^+\pi^-\pi^+\pi^-$  in the GHLS model with the "canonical choice" (21) are shown in Fig. 7 and 8 with the dotted

line. One can see that the simplest variant with the single  $\rho(770)$  s-channel resonance cannot reproduce the data at  $\sqrt{s} \approx 1$  GeV. Upon including the  $\rho'$ ,  $\rho''$  resonances with the couplings chosen by analogy with the  $\rho(770)$  ones one can improve the description of the data [6, 7]. The results of fitting CMD-2 data [6] and the BABAR ones [7] in the fixed width approximation for the  $\rho'$ ,  $\rho''$  resonances with the PDG masses and widths [10] are shown in Fig. 7 and 8. It appears that at  $\sqrt{s} \approx 1$  GeV the joint contribution of the  $\rho'$ ,  $\rho''$  resonances is by the factor of thirty greater than the contribution of  $\rho(770)$ .

**6. Conclusion.** The heavier axial vector resonances  $a'_1$  and  $a''_1$  contributions should be added to the  $a_1(1260)$  one in order to obtain the correct shape of the spectrum in the decay  $\tau \rightarrow 3\pi\nu_\tau$ . Similar problem is found in the vector channel  $e^+e^- \rightarrow \pi^+\pi^-\pi^+\pi^-$ . The contributions of heavier resonances  $\rho'$  and  $\rho''$  are required for correct description of experimental data at energy  $\sqrt{s} \approx 1$  GeV. However, contrary to the case of the vector channel where additional contributions of  $\rho'$  and  $\rho''$  at the above energy exceed the  $\rho(770)$  one, in the axial vector channel  $\tau \rightarrow 3\pi\nu_\tau$ , each of the additional contributions is smaller in magnitude than the contribution of pure GHLS with the single fitted  $a_1$  resonance. See Fig. 2 and 3. But they contribute almost coherently resulting in the acceptable shape of the spectrum and the acceptable magnitude of the branching fraction  $B(\tau^- \rightarrow \pi^+\pi^-\pi^-\nu_\tau) \approx 9\%$ .

## References

- [1] Ulf-G. Meissner, Phys.Rept. **161**, 213 (1988).
- [2] M. Bando, T. Kugo, S. Uehara *et al.*, Phys.Rev.Lett. **54**, 1215 (1985).
- [3] M. Bando, T. Fujiwara, and K. Yamawaki, Progr.Theor.Phys. **79**, 1140 (1988).
- [4] M. Bando, T. Kugo, and K. Yamawaki, Phys.Rept. **164**, 217 (1988). See also review [1].
- [5] S. Schael *et al.* (ALEPH Collaboration), Phys.Rept.**421**, 191 (2005).
- [6] R. R. Akhmetshin, *et al.* (CMD-2 Collab.), Phys.Lett. B**475**, 190 (2000) [arXiv:hep-ex/9912020v1].
- [7] B. Aubert, *et al.* (BaBar Collab.), Phys.Rev. D**71**, 052001 (2005) [arXiv:hep-ex/0502025v1].
- [8] R. Kokoski and N. Isgur, Phys.Rev.D**35**, 907 (1987).
- [9] S. Godfrey and N. Isgur, Phys.Rev.D**32**, 189 (1985).
- [10] C. Amsler, *et al.*, Phys.Lett.**B667**, 1 (2008).
- [11] D. V. Amelin, *et al.*, (the VES Collaboration), Phys. Lett. **B356**, 595 (1995).
- [12] D. Asner, *et al.* (CLEO Collaboration), Phys.Rev.D**61**, 012002(2000) [arXiv:hep-ex/9902022v1].
- [13] M. Zielinski *et al.*, Phys.Rev.Lett. **52**, 1195 (1984).
- [14] N. N. Achasov and A. A. Kozhevnikov, Phys.Rev.D**62**,117503(2000) [arXiv:hep-ph/0007205v2]; Yad.Fiz.**65**,158(2002) [Phys.Atom.Nucl.**65**153(2002)].

Table 1: The values of free parameters of GHLS model obtained from the unconstrained fit of the ALEPH data on the decay  $\tau^- \rightarrow \pi^+\pi^-\pi^-\nu_\tau$  [5] (variant A), and the fit with the constrain  $a = 2$  preserving universality (variant B). Also shown are the corresponding calculated original [3, 4] GHLS parameters and the magnitudes of branching fractions of the above decay.

parameter	variant A	variant B
$m_{a_1}$ [GeV]	$1.332 \pm 0.015$	$1.139 \pm 0.016$
$a$	$1.665 \pm 0.011$	$\equiv 2$
$b$ (calculated)	$1.35 \pm 0.05$	$0.52 \pm 0.03$
$c$ (calculated)	$2.72 \pm 0.08$	$3.74 \pm 0.11$
$d$ (calculated)	$-0.07 \pm 0.03$	$0.54 \pm 0.03$
$\alpha_4$ (calculated)	$-10 \pm 1$	$-27 \pm 2$
$\alpha_5$ (calculated)	$2.82 \pm 0.06$	$1.94 \pm 0.15$
$r$	$0.332 \pm 0.007$	$0.122 \pm 0.006$
$\beta$	$8.5 \pm 0.3$	$15.9 \pm 0.9$
$m_{a'_1}$ [GeV]	$1.59 \pm 0.01$	$1.76 \pm 0.01$
$d'$	$0.99 \pm 0.01$	$1.09 \pm 0.01$
$r'$	$0.96 \pm 0.01$	$0.90 \pm 0.01$
$\beta'$	$0.07 \pm 0.02$	$0.28 \pm 0.02$
$w'$	$\equiv 1$	$\equiv 1$
$\psi'$	$28^\circ \pm 1^\circ$	$48^\circ \pm 1^\circ$
$m_{a''_1}$ [GeV]	$1.88 \pm 0.02$	$2.27 \pm 0.02$
$d''$	$0.46 \pm 0.01$	$0.59 \pm 0.01$
$r''$	$1.45 \pm 0.02$	$1.56 \pm 0.02$
$\beta''$	$0.91 \pm 0.05$	$0.91 \pm 0.03$
$w''$	$1.14 \pm 0.01$	$1.37 \pm 0.01$
$\psi''$	$\equiv 0^\circ$	$\equiv 0^\circ$
$B_{\tau^- \rightarrow \pi^+\pi^-\pi^-\nu_\tau}$	$(9.05 \pm 0.16)\%$	$(9.00 \pm 0.15)\%$
$\chi^2/N_{\text{d.o.f}}$	79/102	70/103

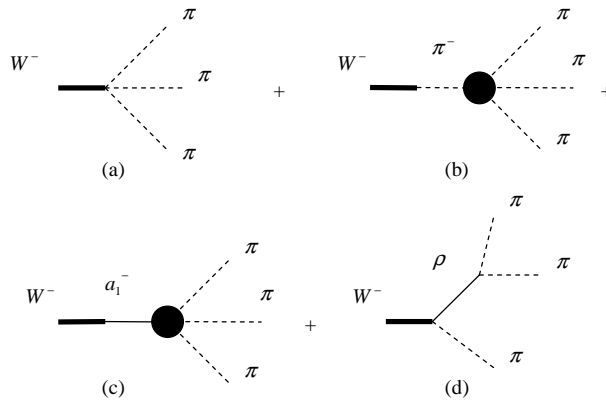


Figure 1: Diagrams schematically describing the transition  $W^- \rightarrow \pi^-\pi^-\pi^+$ . Shaded circles depict the transition including both the point-like and  $\rho$ -exchange contributions. Permutations of pion momenta are understood.



Table 2: The values of free parameters of GHLS model obtained from the fit of the ALEPH data on the decay  $\tau^- \rightarrow \pi^+\pi^-\pi^-\nu_\tau$  [5] constrained in a way as to fix  $a \equiv 2$  and  $\Gamma_{a_1^\pm \rightarrow \pi^\pm \gamma}$ . Variant C is the fit including  $a_1 + a'_1 + a''_1$  contributions. Variant D includes only  $a_1 + a'_1$  ones. Also shown are the corresponding calculated original [3, 4] GHLS parameters and the magnitudes of branching fractions of the above decay.

parameter	variant C	variant D
$m_{a_1}$ [GeV]	$1.368 \pm 0.006$	$1.401 \pm 0.006$
$a$	$\equiv 2$	$\equiv 2$
$b$ (calculated)	$4.89 \pm 0.07$	$5.37 \pm 0.06$
$c$ (calculated)	$1.30 \pm 0.07$	$1.12 \pm 0.05$
$d$ (calculated)	$-0.03 \pm 0.06$	$0.07 \pm 0.04$
$\alpha_4$ (calculated)	$0.66 \pm 0.06$	$0.45 \pm 0.05$
$\alpha_5$ (calculated)	$1.29 \pm 0.10$	$1.31 \pm 0.10$
$r$	$0.790 \pm 0.008$	$0.827 \pm 0.006$
$\beta$ (calculated)	$1.63 \pm 0.12$	$1.58 \pm 0.12$
$\gamma$ [GeV <sup>2</sup> ]	$0.31 \pm 0.01$	$0.35 \pm 0.02$
$m_{a'_1}$ [GeV]	$1.422 \pm 0.007$	$1.513 \pm 0.001$
$a'$	$1.80 \pm 0.03$	$2.01 \pm 0.03$
$r'$	$0.386 \pm 0.005$	$0.370 \pm 0.006$
$\beta'$	$0.96 \pm 0.05$	$0.82 \pm 0.05$
$w'$	$1.19 \pm 0.01$	$1.18 \pm 0.02$
$\psi'$	$\equiv 0$	$39^\circ \pm 1^\circ$
$m_{a''_1}$ [GeV]	$1.800 \pm 0.007$	—
$a''$	$-0.32 \pm 0.02$	—
$r''$	$0.36 \pm 0.02$	—
$\beta''$	$-0.2 \pm 0.2$	—
$w''$	$0.30 \pm 0.04$	—
$\psi''$	$10^\circ \pm 8^\circ$	—
$B_{\tau^- \rightarrow \pi^+\pi^-\pi^-\nu_\tau}$	$(8.97 \pm 0.13)\%$	$(8.96 \pm 0.17)\%$
$\chi^2/N_{\text{d.o.f}}$	45/102	95/107

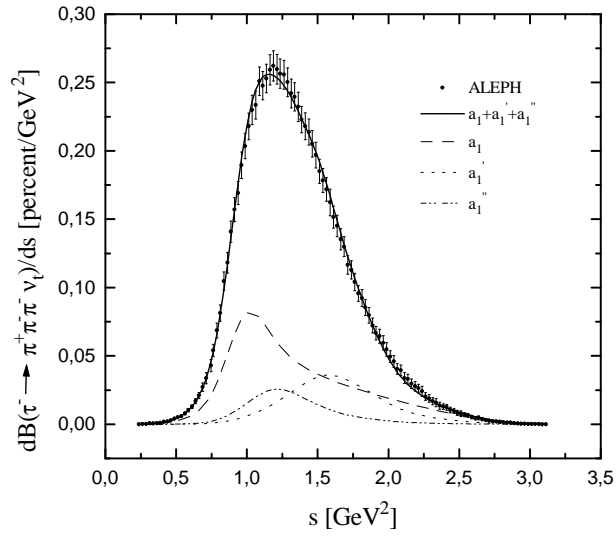


Figure 2: The spectrum of  $\pi^+\pi^-\pi^-$  in  $\tau$  decay in the variant A of the Table 1. The dashed line corresponds to the sum of the diagrams Fig. 1. See the text for more detail.

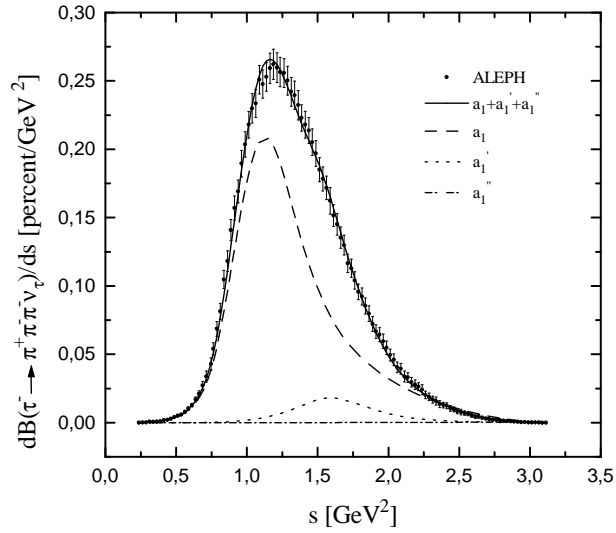


Figure 3: The same as in Fig. 2, but for the parameters of the variant C of the Table 2.

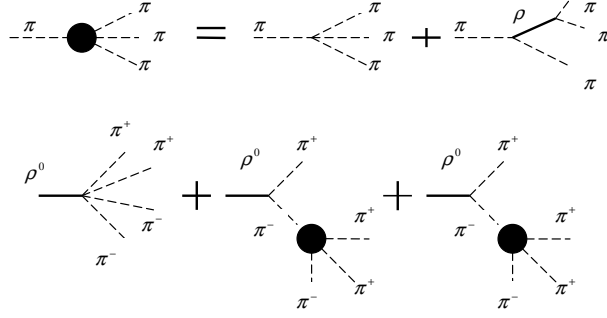


Figure 4: The diagrams due to HLS Lagrangian. Shaded circles in the  $\rho \rightarrow 4\pi$  diagrams stand for the  $\pi \rightarrow 3\pi$  transition shown in the first line of this figure.

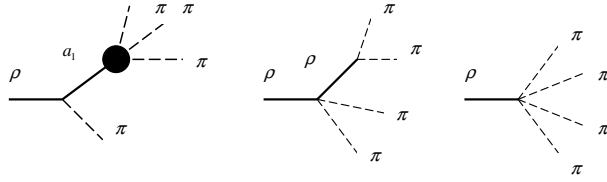


Figure 5: The diagrams due to  $a_1\rho\pi$  and  $\rho\rho\pi\pi$  couplings (GHLS). The shaded circle stands for the total  $a_1 \rightarrow 3\pi$  amplitude similar to Eq. (15).

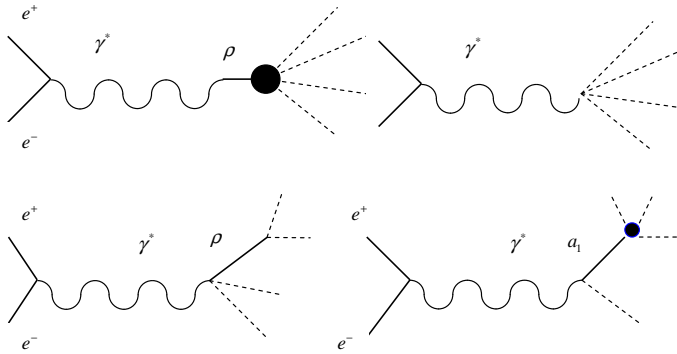


Figure 6: Diagrams describing process  $e^+e^- \rightarrow \pi^+\pi^-\pi^+\pi^-$ . Shaded circle in the first diagram stands for the sum of the  $\rho \rightarrow 4\pi$  diagrams in Fig. 4 and 5. The last three diagrams are due to the point-like  $\gamma \rightarrow 4\pi$ ,  $\gamma \rightarrow a_1\pi$ , and  $\gamma \rightarrow \rho\pi\pi$  couplings from the Lagrangian (17).

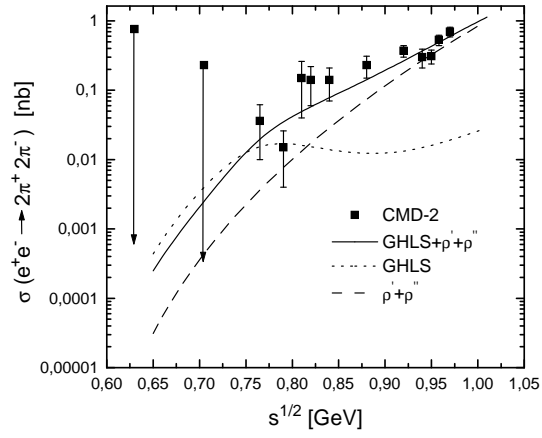


Figure 7: Fitting CMD-2 data [6].

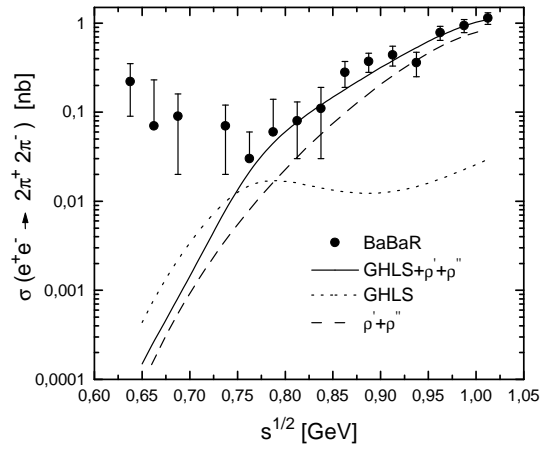


Figure 8: Fitting BaBaR data [7].